Leveraging IoT (Internet of Things) for Reservoir Evaluation in the Oil and Gas Industry

Sivar Qays Ali*

College of Engineering, Department of Petroleum Engineering, Knowledge University 44001 Erbil, Iraq

Abstract. Using IoT (Internet of Things) in reservoir evaluation can significantly enhance the efficiency and accuracy of data collection, monitoring, and analysis in the oil and gas industry. Determining the shale volume distribution is one of the most crucial factors to take into account when evaluating the formation, Since the presence of shale lowers the reservoir's effective porosity and permeability. The volume and distribution of shale and the effective porosity of the formation are estimated utilizing wireline well log data along with Techlog software. The Lower Jurrasic formations are composed of four formations (starting from top to bottom) which are Alan, Mus, Adaiyah and Butmah. In this study, the only studied reservoir formations are Alan, Mus and Adaiyah as provided in the dataset. Shale volume has been calculated by using the gamma ray, the combinations of Neutron-Density and Neutron-Sonic logs were utilized in order to calculate the effective porosities. According to the results, it was concluded that the top of Mus and Adaiyah formations can provide the best reservoir quality and results in comparison with other formations and zones due to the low shale volume and higher effective porosity.

1 Introduction

The oil and gas industry continually seek innovative technologies to improve reservoir evaluation techniques, optimize production processes, and enhance operational efficiency. In recent years, the advent of the Internet of Things (IoT) has revolutionized data collection, monitoring, and analysis in various industries, including oil and gas. This abstract explores the application of IoT in reservoir evaluation, highlighting its potential to transform traditional approaches and deliver significant benefits to the industry.

Shale is a heterogeneous rock that is rich in clay and has a varying content of organic matter and clay minerals, primarily illite, kaolinite, and montmorillonite. Shale is present in the formation has a significant effect on the petrophysical characteristics of the reservoir and lowers its effective and total porosity and permeability [5, 6, 9].

*Sivar Qays Ali : Siver.kais@knu.edu.iq

Furthermore, Gamma ray logs can efficiently give indications about the type of lithology available down in the formation. They are usually known as good indicators of shale existence since shale and shaly formations possess a large amount of radioactive materials. This is why gamma ray logs are usually called shale logs. It is worth mentioning that not every radioactive material is from shale nor every shaly formation would contain high radioactivity [10, 12].

This Paper focuses and sheds light on Internet of Things (IoT) understanding and calculating the shale volume as well as effective porosity for two wells in a carbonate reservoir by utilizing wireline logs data along with using Techlog software to better understand the reservoir evaluation and its impact in oil and gas exploration as well as to understand its contribution in enhancing the quality of reservoir.

1.1 Research Objectives

The main aims of this study are providing the following deliverables:

1. Estimating of shale volume and effective porosity of the studied formation (Alan, Mus and Adaiyah)
2. Calculation of effective porosity.
3. Evaluation of the best interval among the reservoir unit where further evaluations such as core points, fluid samples.
4. Assessment of hydrocarbon bearing zones.

2 Literature Review

[1] stated that well logging is a device which identifies the porosity and permeability of formation as well as their extent and thickness by calculating different physical and chemical properties of the formations. Well logging is a record of formation versus depth and time.

According to [13], the first use of a non-electrical logging tool was from Gamma ray log at which initially presented during 1930s and mainly utilized to differentiate between clean and shaly formation by knowing the intensity of the gamma rays and detecting the concentration of the natural radioactive emissions in formation versus depth. Moreover, the main source of natural radioactivity were the radioactive isotopes associated with Potassium K, Uranium U and Thorium Th. On the other hand, the author claimed that the maximum and minimum gamma ray reading, which represents the clean and shaly formation respectively is useful for shale volume calculation.

According to [7], the amount of radioactivity varies information depends on the age of the rock, as the rock ages less radiation is emitted. Commonly, the shaly formations have more radioactive element and contains higher gamma ray values while sand and carbonates carry low intensity gamma rays. It has been concluded that gamma ray detectors could be developed in order to record the high energy emitted along with the concentration of each component in addition to the number of gamma rays emitted.

[13] advocated that standard gamma ray log could possibly be replaced by the spectral gamma ray in order to assist recognizing the clay type and sort them in terms of the amount of the radioactivity elements such as Thorium Th , Potassium K and Uranium U. In addition, Bassiouni, Z., 1994, stated that spectral gamma ray is a useful contributor in detecting the shale volume information by the response of a very high radioactivity. Moreover, Kowalski,

[16] throughout a study on one of the wells in Oklahoma, it has been observed that in sandstone formation specifically at 570-580 ft, a very high radiation responded on the gamma ray log which was considered as a shale. Nevertheless, with the help of spectrometry log it has been clarified that the high radiation was produced due to the presence of a significant concentration of Uranium in sandstone and eventually been confirmed that this zone is a productive hydrocarbon zone.

In 1950s, a development in definition and evaluation of porosity was done by utilizing neutron log which considered as a first nuclear device measured by the neutron logging tool. The primary principle of this log depended on the fact that the fast and energetic neutrons emitted from the source to the crossed formation could be slowed down by the hydrogen concentration presence information. Interpretation and reading of porosity by using neutron tool reflects the presence of all sources of hydrogen concentration information for instance in shaly formation with the huge amount of bounded water around the clay will significantly affect the log interpretation. Consequently, some concepts have been taken into consideration for instance the tool should be ran in an appropriate way in addition to the use of a suitable correction so that it will have the ability to do a better communication with the hydrogen index within the formation in order to get an accurate and a precise reading of porosity utilizing neutron porosity log tool. [19].

[20] described for the first time the Alan Formation in one of the wells in the North of Mosul with total thickness of around 87 m. The age of Alan formation is identified based on the location which is located in the stratigraphic column that is classified within the lower Jurassic age between middle Jurrassic and Triassic age. However, it has been shown that Alan formation located between Sargelu formation which is located in the middle Jurassic formation and Mus formation located in the lower Jurassic age. On the other hand, the main composition of Alan formation is Predominantly Anhydrite interbedded with Limestones and minor Dolomite.

For the first time Mus formation was defined in one of the wells in Northern Iraq. Nevertheless, the thickness of Mus formation consisted of 50 m of limestone beds. According to lithogy, Mus formation consisted mainly of Limestones with Dolomitic Limestone interbedding. The age of Mus formation is recognized based on the position which is situated in the stratigraphic column categorized within the lower Jurassic age between middle Jurrassic and Triassic age. Additionally, it have been displayed that Mus formation is to be found between Alan formation from the top and Adayiah formation from the bottom which is both located in the lower Jurassic age [12].

Adayiah formation was identified for the first time by [25] in one of the wells in North of Iraq, west of Mosul city [4]. It has been found that the total thickness of Adyiah formation was 90 m, consisting of anhydrite, limestone and shale [6]. According to the master log it has been seen that Adayiah formation consisted of Predominantly of dolomitic Limestone, with minor Shale & Anhydrite interbedding & occasional softer marly bands, all appearing in the lower half. However, the age of Adyiah formation is identified as shown in the master log that is situated in the stratigraphic column which is categorized within the lower Jurassic age between middle Jurrassic and Triassic age.
While Adyiah formation situated between Mus formation from the top and Butmah formation from the bottom is both located in the lower Jurassic age.

3 Materials and Methods

3.1 Materials

In this paper conventional well logs data are obtained in at least Two wells which are available in LAS files. However, the well log data are ready to be utilized with the software in order to calculate the required parameters along with their methods. This Study requires using of software along with the data combined in order to study the characteristics of a fractured carbonate reservoir. Due to Privacy restrictions of the obtained data which belongs to a selected field in Kurdistan Region, the name of the field has been changed to X field as well as the name of the wells changed to Well-A and Well-B.

3.2 Methods

In this study, Techlog software is used to calculate Vsh and porosity from gamma ray and combination of neutron-density and neutron-sonic logs respectively.

Gamma ray log is utilized in order to calculate the volume of shale in reservoir. However, this method calculates the shale volume with a gamma ray curve as an input. The very first step in order to calculate the Vsh is to calculate the gamma ray index GR_{index} as shows in equation (1) [33].

$$I_{GR}\frac{GR_{log} - GR_{min}}{GR_{max} - GR_{min}} \quad (1)$$

Where I_{GR} is Gamma Ray Index, GR_{min} is Minimum gamma Ray reading which is called matrix, GR_{max} is Maximum gamma Ray reading which is called shale.

in this study the values of shale volume have been calculated by two methods Larinov (Older rocks method). the values of calculated shale volume from

Larinov (Older rocks) method is shown in the equation (2) [33]

$$V_{sh} = 0.33 \times (2^{2.1 \times I_{GR}} - 1) \quad (2)$$

However, regarding the calculation of effective porosity from Neutron-Density derived porosity, corrections need to be taken into consideration and should be made based on the matrix density and the actual lithology of the formation.

The first step is to calculate the corrected Density porosity $Ø_d$ by utilizing the log track and equation method as shown in equation (3) [33].

$$Ø_{d\ corrected} = \frac{\rho_{ma} - \rho_b}{\rho_{ma} - \rho_f} \quad (3)$$

Where; $Ø_d$ or DPHI is the density derived porosity, ρ_{ma} is matrix density, ρ_f is fluid density, ρ_b or RHOB is formation bulk density (from the log reading).

ρ_b could be taken from the log track which is the RHOB from the log reading, regarding the ρ_{ma} and ρ_f.

the effective porosity could be calculated using equation (4) [33].

$$Ø_E = Ø_T\,(1 - V_{sh}) \tag{4}$$

Where $Ø_{T\ is}$ Total porosity from Neutron Density log, $Ø_{E\ is}$ Effective porosity from Neutron Density log, $Ø_{N\ is}$ Derived porosity from Neutron log, $Ø_{D\ is}$ Porosity from Density log, $V_{sh\ is}$ Shale volume.
sonic porosity can be calculated from the Δt (Transient time) from the log track and using the Wyllie equation as presented in equation (5) [33].

$$Øs = \frac{\Delta t_{log} - \Delta t_{ma}}{\Delta t_{fl} - \Delta t_{ma}} \tag{5}$$

Where Δt_{log} is the interval transient time in the formation, Δt_{ma} is the interval transient time in the matrix , Δt_{fl} is the interval transient time in the fluid inside the formation (fresh water=189 µsec/ft, salt water mud=185 µsec/ft).

4 Data Analysis

4.1 Shale volume

4.1.1 In Well A and Well B

As Shown in (fig-1) below by using Techlog software and analyzing the data, high volume of shale represented in Alan and Adaiyah formation more than in Mus formation in both wells A and B.

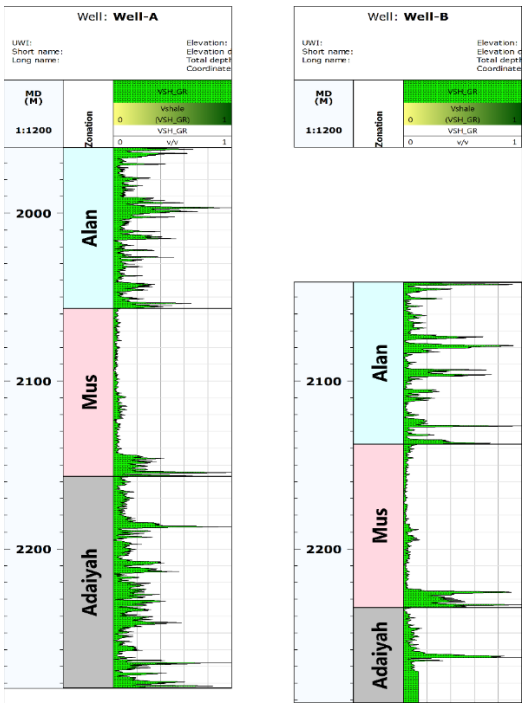

Fig. 1. Shows the calculated shale volume logs from gamma ray log utilizing Larinov (Older rocks) method for both wells A&B in Lower Jurassic formation for X field

4.2 Effective Porosity

4.2.1 In Well A and Well B

As Shown in (fig-2) below by using Techlog software and analyzing the data, high effective porosity represented in top of Mus and Adaiyah formation more than Alan formation in both wells A and B.

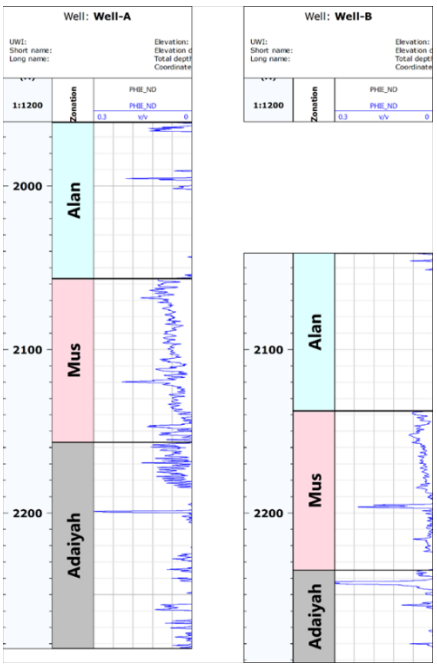

Fig. 2. Effective porosity derived from Neutron-Density and Neutron-Sonic logs for both wells A&B.

5 Results and Discussions

5.1 Shale Volume

5.1.1 Well A

In well A a random distribution of shale volume has been shown in Alan formation starting from 15% at very top of Alan A1 then a small increasing occurs in A2 with 20% of shale, A3 shows 14% of shale content while A4 and A5 having 10% and 18% of shale volume respectively. However, the average shale volume in Alan formation in well A is 15%. According to Mus formation the shale volume Vsh is increasing bit by bit as moving downward starting from M1 and M2 which only 3%.

In Adaiyah formation there is an unstable distribution of shale volume and maximizing as moving downward in shale volume as it has 10% of shale in very top of Adaiyah AD1. there is a very high shale content in the very base of Adaiyah which is equal to almost 26% of shale shown.

Table 1. Shows the calculated values of shale volumes by Older Rocks method for well A for each of formation zones.

Well A							
Formation	**Zone**	**Top (MD)**	**Bottom (MD)**	**Thickness (M)**	**Formation Thickness**	**Vsh OR**	**Formation Vsh**
Alan	A1	1961	1981	20	95.8	0.15	0.15
Alan	A2	1981	2001	20		0.2	
Alan	A3	2001	2021	20		0.14	
Alan	A4	2021	2041	20		0.1	
Alan	A5	2041	2056.8	15.8		0.18	
Mus	M1	2056.8	2076	19.2	100	0.03	0.056
Mus	M2	2076	2096	20		0.02	
Mus	M3	2096	2116	20		0.04	
Mus	M4	2116	2136	20		0.04	
Mus	M5	2136	2156.8	20.8		0.15	
Adaiyah	AD1	2156.8	2176	19.2	126.2	0.1	0.17
Adaiyah	AD2	2176	2196	20		0.15	
Adaiyah	AD3	2196	2216	20		0.17	
Adaiyah	AD4	2216	2236	20		0.2	
Adaiyah	AD5	2236	2256	20		0.16	
Adaiyah	AD6	2256	2276	20		0.15	
Adaiyah	AD7	2276	2283	7		0.26	
						Avg Vsh = 0.13	

5.1.2 Well B

In well B a random distribution of shale content is shown in Alan formation starting from 10% at very top of Alan A1 at that point a slight increasing occurs in A2 and A3 with 12% and 11% of shale volume respectively However, the average shale volume in Alan formation in well B is 11%. According to Mus, the top and middle part of Mus shows a very clean shale distribution which there is only 4% and 2% of shale volume in M1 and M2 respectively. The average shale volume in Mus in well B is 6% only. However, the average shale volume Vsh in Adaiyah formation in well B is equal to 10% only, while the average shale content in all well B is 9%.

Table 2. The calculated values of shale volumes by Older Rocks Method for well B for each of formation zones

Well B							
Formation	**Zone**	**Top (MD)**	**Bottom (MD)**	**Thickness (M)**	**Formation Thickness**	**Vsh OR**	**Formation Vsh**
Alan	A1	2041	2061	20	96.6	0.1	0.11
Alan	A2	2061	2081	20		0.12	
Alan	A3	2081	2101	20		0.11	
Alan	A4	2101	2121	20		0.07	
Alan	A5	2121	2137.6	16.6		0.14	
Mus	M1	2137.6	2157	19.4	97.4	0.04	0.06
Mus	M2	2157	2177	20		0.02	
Mus	M3	2177	2197	20		0.04	
Mus	M4	2197	2217	20		0.03	
Mus	M5	2217	2235	18		0.2	
Adaiyah	AD1	2235	2255	20	56	0.06	0.1
Adaiyah	AD2	2255	2275	20		0.11	
Adaiyah	AD3	2275	2291	16		0.13	
						Avg Vsh = 0.09	

Table (3) shows the average shale volume for well A and B for each formation zones (Alan, Mus and Adaiyah). However, Alan and Adaiyah formation having the highest shale volume with 13% of shale compared to Mus formation which has the lowest shale content which is equal to only 6% only

Table 3. The average shale volume for well A and well B for each formation zone

Formation	Well A	Well B	Avg Vsh
Alan	0.15	0.11	0.13
Mus	0.06	0.06	0.06
Adaiyah	0.17	0.1	0.13

5.2 Effective porosity

5.2.1 Effective Porosity in Alan Formation in well A

In well A, by Utilizing Neutron Density and Neutron Sonic methods, we can notice that the derived porosity is higher than in case of Neutron Sonic method. Eventually, the average final effective porosity in Alan formation found to be 0.1% in well A.

Table 4. The values of effective porosity in Alan Formation in well A

Well A							
Formation	**Zone**	**Top (MD)**	**Bottom (MD)**	**Thickness (M)**	**Ø N-D (eff.)**	**Ø N-S (eff.)**	**Final Ø (eff.)**
Alan	A1	1961	1981	20	0.01	0.004	0.004
Alan	A2	1981	2001	20	0.01	0	0
Alan	A3	2001	2021	20	0.002	0.001	0.001
Alan	A4	2021	2041	20	0	0	0
Alan	A5	2041	2056.8	15.8	0.003	0	0
Alan Formation	**1961**	**2056.8**	**95.8**	**0.006**	**0.001**	**0.001**	

5.2.2. Effective Porosity in Alan Formation in well B:

The average final effective porosity in Alan formation found to be 0.1% in well B.

Table 1. The values of effective porosity in Alan Formation in well B

Well B							
Formation	**Zone**	**Top (MD)**	**Bottom (MD)**	**Thickness (M)**	**Ø N-D (eff.)**	**Ø N-S (eff.)**	**Final Ø (eff.)**
Alan	A1	2041	2061	20	0.003	0.003	0.002
Alan	A2	2061	2081	20	0	0.001	0
Alan	A3	2081	2101	20	0	0	0
Alan	A4	2101	2121	20	0	0	0
Alan	A5	2121	2137.6	16.6	0	0	0
Alan Formation	**2041**	**2137.6**	**96.6**	**0.001**	**0.001**	**0.001**	

5.2.3 Effective Porosity in Mus Formation in well A

In well A, the top of Mus formation has good porosity while the bottom lack porosity. the effective porosity by Neutron Density method records higher again than in case of Neutron-Sonic combination method, In M1 it reads 8% and then declining gradually to 6% and 3% in M4 and M5 respectively while in N-S starts from 6% decreasing to 5%, 4% and 1 % in M2, M4 and M5 respectively. However, the average Final effective porosity in Mus formation reads only 4% for the thickness of 100 meter

Table 2. The values of effective porosity in Mus Formation in well A

Well A							
Formation	**Zone**	**Top (MD)**	**Bottom (MD)**	**Thickness (M)**	**Ø N-D (eff.)**	**Ø N-S (eff.)**	**Final Ø (eff.)**
Mus	M1	2056.8	2076	19.2	0.08	0.06	0.06
Mus	M2	2076	2096	20	0.06	0.05	0.05
Mus	M3	2096	2116	20	0.06	0.04	0.04
Mus	M4	2116	2136	20	0.06	0.04	0.04
Mus	M5	2136	2156.8	20.8	0.03	0.01	0.01
Mus Formation	**2056.8**	**2156.8**	**100**	**0.06**	**0.04**	**0.04**	

5.2.4 Effective Porosity in Mus Formation in well B

In well B, the top of Mus formation has good porosity while the bottom lack porosity. the value of derived effective porosity by Neutron Sonic method records higher than in case of Neutron-Density combination method, In M1 it reads 4% and then declining gradually to 3% , 1% and then to 0.7% in M3, M4 and M5 respectively while in N-S starts from 5% declining to 2%, 1% in M2, M4 and M5 respectively. However, the average Final effective porosity in Mus formation in well B records only 2% for the thickness of 97.4 meter.

Table 3. The values of effective porosity in Mus Formation in well B

Well B							
Formtion	**Zone**	**Top (MD)**	**Bottom (MD)**	**Thickness (m)**	**Ø N-D (eff.)**	**Ø N-S (eff.)**	**Final Ø (eff.)**
Mus	M1	2137.6	2157	19.4	0.04	0.05	0.04
Mus	M2	2157	2177	20	0.03	0.04	0.03
Mus	M3	2177	2197	20	0.03	0.05	0.02
Mus	M4	2197	2217	20	0.01	0.02	0.01
Mus	M5	2217	2235	18	0.007	0.01	0.007
Mus Formation	**2137.6**	**2235**	**97.4**	**0.02**	**0.03**	**0.02**	

5.2.5 Effective Porosity in Adaiyah Formation in well A

For Adaiyah formation, the values calculated by N-D methods looks much higher than in N-S method, where it starts by 5% in AD1 decreasing to 2%, 1% in zones AD6 and AD7 respectively, while in N-S method it starts from 2.4% decreasing gradually to until it reads 1% and 0.4% in AD6 and AD7 respectively. Eventually, the final average effective porosity for the Adaiyah formation in well A could reads 0.7% only for the thickness of 126.2 meter

Table 4. The values of effective porosity in Adaiyah Formation in well A

Well A							
Formtion	**Zone**	**Top (MD)**	**Bottom (MD)**	**Thickness (M)**	**Ø N-D (eff.)**	**Ø N-S (eff.)**	**Final Ø (eff.)**
Adaiyah	AD1	2156.8	2176	19.2	0.05	0.024	0.02
Adaiyah	AD2	2176	2196	20	0.02	0.007	0.005
Adaiyah	AD3	2196	2216	20	0.01	0.005	0.004
Adaiyah	AD4	2216	2236	20	0.01	0.004	0.003
Adaiyah	AD5	2236	2256	20	0	0.002	0.001
Adaiyah	AD6	2256	2276	20	0.02	0.013	0.013
Adaiyah	AD7	2276	2283	7	0.01	0.004	0.003
Adaiyah Formation	**2156.8**	**2283**	**126.2**	**0.02**	**0.01**	**0.007**	

5.2.6 Effective Porosity in Adaiyah Formation in well B

In well B, the calculated derived effective porosity by N-S method looks higher than in N-D method, it starts from 11% in AD1 and AD2 increasing to 13% in AD3, while in N-D method it starts from 5% in AD1 decreasing to 0.6% in AD3. Eventually, the final average effective porosity for the Adaiyah formation in well B reads 3% only for the thickness of 56 meter

Table 5. The values of effective porosity in Adaiyah Formation in well B

Well B							
Formation	**Zone**	**Top (MD)**	**Bottom (MD)**	**Thickness (M)**	**Ø N-D (eff.)**	**Ø N-S (eff.)**	**Final Ø (eff.)**
Adaiyah	AD1	2235	2255	20	0.05	0.11	0.03
Adaiyah	AD2	2255	2275	20	0.006	0.11	0.007
Adaiyah	AD3	2275	2291	16	0.006	0.13	0.06
Adaiyah Formation	**2235**	**2291**	**56**	**0.02**	**0.12**	**0.03**	

6 Conclusions

The top three zones of Mus formation have a very low shale contents compared to other zones with an average of 3% in both wells A and B. Higher values of effective porosity and permeability were observed in the top three zones of Mus formation with an average value of 5% in well-A and 3% in well-B. As well as higher permeability values compared to other zones with 8 mD and 9 mD in well-A and well-B respectively.

The top three zones of Mus formation M1, M2 and M3 as well as the top three zones of Adaiyah formation AD1, AD2 and AD3 were recognized to act as a good reservoir due to the low shale volume, better porosity and permeability values, and very good oil saturation values. The top three zones of Adaiyah formation had higher shale contents than Mus with 14% in well-A and 10% in well-B.

The values of effective porosity in the top three zones of Adaiyah formation was found to be 1% in well-A and 5% in well-B.

The Autor would like to thank Asst. Prof. Dr. Ali Kattan, Editor-in-Chief, for his continuous support, guide and follow up.

References

1. Alger, R. P., Geological use of wireline logs: in Developments in Petroleum Geology-2. Applied Science Publisher, **2**(2), pp. 207-272 (1980)
2. Allioli, F., Nicoletti, L., Stoller, C., & Xu, L, Natural Gamma Ray Tool Response Discrepancies: Not Always Due to the Calibration! Society of Petroleum Engineers. doi:10.2118/191669-MS (2018)
3. Alger, R. P., Geological use of wireline logs: in Developments in Petroleum Geology-2. Applied Science Publisher, **2**(2), pp. 207-272 (1980)
4. Alimoradi, A., Moradzadeh, A. and Bakhtiari, M., 2011. Methods of water saturation estimation: Historical perspective. Journal of Petroleum and Gas Engineering, 2(03), pp.45-53.
5. Archie, G.E., The electrical resistivity log as an aid in determining some reservoir characteristics: Journal of Petro¬leum Technology, v. **1**, p. 55−62 (1942)
6. Asquith, G.B., Combining Water Saturation/Ratio Method, Moveable Hydrocarbon Index, Bulk Volume Water And Archie Water Saturation. American Association of Petroleum Geologists, pp.22-28 (1985)
7. Bassiouni, Z., Theory, Measurement, And Interpretation Of Well Logs. 1st ed. United States of America: Henry L. Doherty Memorial Fund of AIME, Society of Petroleum Engineers, pp.1-200 (1994)
8. Chatterjee, R., Datta Gupta, S. and Pratim Mandal, P., Fracture and Stress Orientation from Borehole Image Logs: A Case Study from Cambay Basin, India. JOURNAL GEOLOGICAL SOCIETY OF INDIA, 89, pp.573-580 (2017)
9. Chen, M.-Y., Habashy, T. M., Mariana, D. R., Schroeder, R. J., & Taherian, M. R. Spontaneous Potential: Laboratory Experiments and Modeling Results. Society of Petro-physicists and Well-Log Analysts (1995)
10. Clavier, C., Coates, G., and Dumanoir, J., Theoretical and Experimental Bases for the Dual-Water Model for Interpretation of Shaly Sands, SPE Journal- 24 (2), pp. 153-168 (1984)
11. Dandekar, A.Y., Petroleum Reservoir Rock and Fluid Properties. 2nd ed. Boca Raton: Taylor & Francis Group, pp.1-500 (2013)

12. Edmundson, H. et al, The Sound of Sonic: A Historical Perspective and Introduction to Acoustic Logging. Canadian Society of Exploration Geophysicists, 34(5) (2009)
13. Ellis, V. & Singer, M., Well Logging For Earth Scientists. 2nd ed. Netherland: Springer, pp.351-530 (2007)
14. Ellis, D., Formation Porosity Estimation from Density Logs. Society of Petro-physicists and Well-Log Analysts (2003)
15. Ezekwe, N., Petroleum Reservoir Engineering Practice. 1st ed. Pearson, pp.2-4 (2010)
16. Gartner, J. & Suau, J., Fracture Detection from Well Logs. Society of Petrophysicists and Well-Log Analysis, 21(02), pp.1-11 (1980)
17. Glover, P.W.J., MSc Notes in Petroleum Geology. Department of Geology and Petroleum Geology University of Aberdeen UK (2000)
18. Heflin, J. D., 1979. Fracture Detection in West Coast Reservoirs Using Well Logs. Society of Petroleum Engineers (1979)
19. Heslop, A., Gamma-Ray Log Response of Shaly Sandstones. Society of Petro-physicists and Well-Log Analysts (1974)
20. Hubbert, M., Natural and Induced Fracture Orientation. American Association of Petroleum Geologists, pp.235-237 (1972)
21. Kowalski, J.J. & Asekun, S. O., It May Not Be Shale. SPWLA 20th Annual Logging Symposium, Tulsa, Oklahoma (1979)
22. Lander, L. A., Silva, A., & Simon, C., Resistivity Logging in Conductive-Mud Environment and High Resistivity Formations. Dual Laterolog or Propagation LWD Tool? Society of Petroleum Engineers. doi:10.2118/177084-MS (2015)
23. Lambertini, R., Fracture Identification and Quantification Using Borehole Images: Maracaibo Basin, Venezuela. Society of Petroleum Engineering, pp.89-95 (1992)
24. Laongsakul, P. and Dürrast, H., Characterization of reservoir fractures using conventional geophysical logging. Songklanakarin Journal of Science And Technology (SJST), 33(2), pp.237-246 (2011)
25. Lee, Myung W., Connection equation and shaly-sand correction for electrical resistivity: U.S. Geological Survey Scientific Investigations Report 2011–5005, **9** (2011)
26. Maxwell, S. C., Hydraulic Fracture Height Growth. Canadian Society of Exploration Geophysicists, 36(09), pp.19-22 (2011)
27. Nichols, G., Sedimentology and Stratigraphy. 2nd ed. United States: Gary Nichols, pp.1-400 (2009)
28. Osoba, J., Gist, R., & Carroll, H., Porosity Determination From The Density Log In Western Gas Sands. Society of Petro-physicists and Well-Log Analysts (1980)
29. Peeters, M. & Hartley, R., Induced Fracture Height Detection From Wireline Logs. Society of Petropysicists and Well-log Analysts, pp.1-7 (1984)
30. Pickett, G. R., Evaluation of Fractured Reservoir. Society of Petroleum Engineers Journal, 9(01), pp.28-38 (1969)
31. Plumb, R.A. and S.H. Hickman ., Stress-induced borehole enlargement: a comparison between the four-arm dipmeter and the borehole televiewer in the Auburn geothermal well. - J. Geophys. Res., 90, 5513-5521 (1985)
32. Poupon, A. and Leveaux, J., Evaluation of Water Saturation in Shaly Formations, Society of Petrophysicists and Well-Log Analysts (1971)
33. Serra, O., Fundamentals Of Well-Log Interpretation. 1st ed. New York: Elsevier Science Publishing (1984)